Introduction

Acute myeloid leukemia (AML) is a clonal malignant hematopoietic disease characterized by a block in differentiation, resulting in accumulation of immature myeloid cells.[1,2] Karyotypic analyses have revealed several frequent chromosomal translocations producing fusion genes associated with AML. The t(8;21)(q22;q22) translocation is one of these abnormal karyotypes, and this translocation produces *AML1-ETO* fusion products.[3,4] The *AML1-ETO* blocks hematopoietic differentiation and enhances self-renewal of human and murine hematopoietic stem cells.[5,6] The fusion product apparently binds to *AML1* target genes and represses their transcription.[3,6] The inv(16)(p13q22) or t(16;16)(p13;q22) produces the leukemogenic *CBFB-MYH11* fusion gene which blocks differentiation of hematopoietic stem cells by inhibiting the function of *AML1*.[7,8] Acute promyelocytic leukemia cells usually have t(15;17)(q22;q11-21) producing *PML-RARA* fusion products which also behave as a transcriptional repressor.[9,10] Other frequent translocations include t(9;11), t(6;11), inv(3)/t(3;3) and t(6;9).[11] Trisomy 8, 11, 13, 21 and 22, and deletion of chromosome 5/5q, 7/7q, 17/17p and 20/20q also occur moderately frequently.[2,11,12] About 45-50% of AML patients have no detectable chromosomal abnormalities.[13,14] In general, these individuals with a normal karyotype in their leukemic cells show an intermediate prognosis.[13,14]

Besides chromosomal abnormalities, the leukemic cells can have a variety of mutations involving individual genes. Activating mutations of the receptor tyrosine kinase, FMS-like tyrosine kinase 3 (*FLT3*) occur in about 30% AML patients; two major mutant forms occur: an internal tandem duplication (ITD) or a point mutation in the tyrosine kinase domain (TKD).[15] Activating mutations at codon 12, 13 or 61 of either the *NRAS* or *KRAS* occur in 25% and 15% of AML patients, respectively.[1,16] About 10-15% of AML samples have inactivating mutations of C/EBPα whose wild-type function is to enhance differentiation.[17,18] Nucleophosmin1 (NPM1) is mutated in 50-60% of AML samples with normal karyotype.[13,19] This protein has an important role in ribosome biogenesis, including nuclear export of ribosomal proteins. Mutant NPM1 has an aberrant nuclear export signal and remains localized in the cytoplasm.[20]

Single-nucleotide polymorphism microarray (SNP-chip) analysis is a new technique to examine the genome including any copy-number changes and loss of heterozygosity (LOH).[21-25] Importantly, SNP-chip analysis can reveal cryptic abnormalities such as a small copy-number changes (< 10 Mb) or copy-number neutral loss of heterozygosity [CNN-LOH, also called uniparental disomy (UPD)] that cannot be detected by karyotype analysis. In addition, comparative genomic hybridization cannot detect CNN-LOH. SNP-chip analysis has been used in chronic lymphocytic leukemia,[24,25] childhood acute lymphoblastic leukemia,[26,27] juvenile myelomonocytic leukemia,[22] follicular lymphoma,[23] multiple myeloma,[20] and AML.[21,22,26-34]

In the present study, we identified hidden abnormalities and novel disease-related genomic regions using 250 K SNP-chip analysis in samples from patients with normal karyotype AML/myelodysplastic syndrome (MDS). The use of CNAG (copy-number analysis for Affymetrix GeneChips) program[21] and a new algorithm AsCNAR (allele-specific copy-number analysis using anonymous references)[23] provided a highly sensitive technique to detect CNN-LOH, as well as, copy-number changes in AML/MDS genomes.

Design and Methods

Patients' samples

Samples from 30 anonymized patients with normal karyotype AML and 8 anonymized patients with normal karyotype MDS (age, 33-88 years; median, 62 years) were examined. These samples were isolated from bone marrow at diagnosis. The patients' age, gender, diagnosis, white blood cell count (WBC), karyotype and additional mutations of *FLT3* and *NPM1* are summarized in Table 1. This study was approved by Cedars-Sinai Medical Center (IRB number 4485).

High-density SNP-chip analysis

Genomic DNA was isolated from AML/MDS cells, and the DNA was subjected to GeneChip Human mapping 250 K array NspI microarray (SNP-chip, Affymetrix, Santa Clara, CA, USA) as described previously.[21,25] Hybridization, washing and signal detection were performed on GeneChip Fluidics Station 400 and GeneChip scanner 3000 according to the manufacturer's protocols (Affymetrix). Microarray data were analyzed for determination of both total and allelic-specific copy-number using the CNAG program as previously described[21,23] with minor modifications; the status of copy-numbers as well as CNN-LOH at each SNP was inferred using the algorithms based on hidden Markov models.[21,23] GNAGraph software was used for clustering of AML samples with regards to their copy-number changes, as well as CNN-LOH.[27] Size, position and location of genes were identified with UCSC Genome Browser *http://genome.ucsc.edu*. Copy-number changes, including duplication and deletion, were identified by allele-specific CNAG software.[23,27] These copy-number changes include copy-number variant and physiological deletion at the immunoglobulin and T-cell receptor genes. Copy-number variants as described previously at *http://projects.tcag.ca/variation* and physiological deletions were eliminated manually, and other regions detected by allele-specific CNAG software are listed on Table 4.

Fluorescence in situ hybridization analysis

Bone marrow samples from AML patients were used for interphase fluorescence *in situ* hybridization (FISH) analysis. The FISH studies were performed using the following probes: D5S721 (5p15.2), D5S23 (5p15.2), D7Z1 (centromere of chromosome 7), ABL (9q34.12), EGR1 (5q31.2), D7S486 (7q31), TP53 (17p13.1), D8Z2 (centromere of chromosome 8), AML1 (21q22.12) and BCR (22q11.23) (ABBOTT/VYSIS, Des Plaines, IL, USA). Probes for the 12p13 region [fluorescein-labeled ETV6-

downstream region (483 kb-length) and Texas-red-labeled ETV6-upstream region (264 kb-length)] were used for FISH analysis in case #5. The ETV6 probes were obtained from ABBOTT/VYSIS.

Determination of SNP sequences, JAK2, FLT3, NPM1, and AML1/RUNX1 mutations, and other target genes in cases of CNN-LOH

To determine the SNP sequences, (SNP identities are rs7747259, rs1122637, rs9505293, rs6934027, rs280153 and rs191986) in case #38 chromosome 6p region, the genomic region of each SNP site was amplified by genomic polymerase chain reaction (PCR) using specific primers. For determination of *JAK2* V617F mutation in case #20, genomic PCR was performed with specific primers. PCR products were purified and sequenced. The sequences of the primers are shown in *Online Supplementary Tables S1 and S2*. To determine the *FLT3*-ITD mutation, the PCR reaction was performed with specific primers, and the PCR products were separated on a 2.0% agarose gel stained with ethidium bromide as described previously[34,35] Mutations at exon 12 of the *NPM1* gene were determined using a melting curve-based LightCycler assay (Roche Diagnostics, Mannheim, Germany).[36] Denaturing high-performance liquid chromatography analysis was performed to determine the *AML1/RUNX1* mutation in case #17 as described previously.[37] Alterations of several tyrosine kinase genes including *FGR* (case #3 and #23), *DDR1* (case #2 and 38), *TYK2* (case #2), *MATK* (case #2), *FER* (case #8) and *FGFR4* (case #8) were determined by either nucleotide sequencing of their exons and/or band-shifts of PCR products of exons after their electrophoresis and visualization on a gel (single strand conformation polymorphism), as described previously[38] with minor modifications. The PCR reaction contained genomic DNA, 500 nM of each of the primers, 200 nM of each of the dNTP, 0.5 units of Taq DNA polymerase and 3 μCi [α-32P] dCTP in 20 μL PCR products were diluted 10-fold in the loading buffer (10 mM NaOH, 95% formamide, and 0.05% of both bromophenol blue and xylene cyanol). After denaturation at 94°C for 5 min, 2 mL of the samples were loaded onto a 6% non-denaturating polyacrylamide mutation detection enhancement gel (Bioproducts, Rockland, ME, USA) with 10% (v/v) glycerol and separated at 300 V for 20 h. The gel was dried and subjected to autoradiography.

Table 1. **Baseline clinical characteristics of 38 cases of normal karyotype acute myeloid leukemia/myelodysplastic syndrome.**

Group	Case #	Gender	Age	Type	WBC x10⁹/L	*FLT3*	*NPM1*	Karyotype
A	29	M	49	AML M0	13.8	–	–	46,XY
	1	F	33	AML M1	3.5	–	–	46,XX
	14	M	43	AML M1	27.9	–	–	46,XY
	15	F	67	AML M1	365	–	+	46,XX
	6	M	66	AML M2	2.5	–	–	46,XY
	24	M	88	AML M2	6.3	–	–	46,XY
	25	F	61	AML M2	11.9	–	+	46,XX
	33	F	60	AML M2	24.5	+	+	46,XX
	44	M	65	AML M2	62.8	–	–	46,XY
	18	F	43	AML M4	43.1	–	+	46,XX
	19	M	37	AML M4	209	–	+	46,XY
	32	M	45	AML M4	9.5	–	+	46,XY
	34	F	80	AML M4	71.1	+	–	46,XX
	31	F	45	AML M5b	12.7	+	+	46,XX
	16	F	77	MDS RA	5.3	–	–	46,XX
	35	F	68	MDS CMML-1	5.6	–	–	46,XX
	36	F	69	MDS RAEB-1	4.6	–	–	46,XX
	39	F	74	MDS RAEB-1[1]	5.4	–	–	46,XX
	42	F	79	MDS	3.2	–	–	46,XX
B	10	F	49	AML M1	17.0	+	–	46,XX
	4	M	76	AML M2	2.3	–	–	46,XY
	5	F	67	AML M2	1.1	–	–	46,XX
	8	F	75	AML M2	1.8	–	–	46,XX
	9	M	65	AML M2	48.3	–	–	46,XY
	17	M	78	AML M2	1.1	–	–	46,XY
	20	F	65	AML M2	34.3	–	–	46,XX
	23	M	69	AML M2	2.0	–	+	46,XY
	26	M	36	AML M2	14.2	–	+	46,XY
	2	F	71	AML M4	1.9	–	+	46,XX
	7	F	85	AML M4	2.4	–	–	46,XX
	21	F	38	AML M4	37.6	+	+	46,XX
	38	M	53	AML M4	40	+	+	46,XY
	3	F	67	AML M5b	56	+	+	46,XX
	37	F	65	AML M5b	72.8	+	+	46,XX
	12	M	69	MDS RA	11.5	–	–	46,XY
	41	M	77	MDS RA[1]	7.1	–	–	46,XY
	13	F	54	MDS RAEB-2	–	–	–	46,XX
	11	F	60	t-AML M2	1.7	–	–	46,XX

t-AML: therapy-related AML; RA: refractory anemia; RAEB-1 or -2: refractory anemia with excess blasts subtype-1 or -2; CMML: chronic myelomonocytic leukemia; [1]new WHO classification.

Quantitative real-time polymerase chain reaction

Gene-dosages of chromosome 6p24.3 in case #38, and the *MYC* and *CDKN2A* genes in case #20 were determined by quantitative real-time PCR (iCycler, Bio-Rad, Hercules, CA, USA) using Sybr Green. To determine the relative gene dosage of each sample, the chromosome 2p21 region was measured as a control.[27] The copy-number of the 2p21 region was normal, as determined by SNP-chip analysis, in these samples. The delta threshold cycle value (ΔCt) was calculated from the given Ct value by the formula ΔCt = (Ct sample - Ct control). The fold change was calculated as $2^{-\Delta Ct}$. Primer sequences are shown in *Online Supplementary Table S2*.

Gene expression microarray analysis

Total RNA was isolated from AML/MDS cells and processed according to Affymetrix guidelines for analysis with HGU133 Plus 2.0 microarrays. Data were analyzed with R version 2.5.0 using Bioconductor version 2.0.[39] Data were normalized using the robust multi-array average procedure.[40] Since most regions that showed chromosomal abnormalities were not recurring, we were not able to compare individual genes across samples with statistical tests. To assess plausibility of large deletions and amplifications, we subtracted

from each gene (in the respective region) mean expression of this gene in other cases: case #11 was compared with 37 normal karyotype AML/MDS cases; and cases #20, #4 and #5 were compared with other normal karyotype AML/MDS samples. We then calculated a mean expression difference for each region and considered a value below zero to be consistent with deletion and a value above zero to be consistent with amplification.

Results

Proof of principal

To identify hidden abnormalities in AML/MDS with a normal karyotype, 37 samples were analyzed by 250K SNP-chip microarray. One additional case (case #11) had only 13 metaphases and chromosomal abnormalities were not detected on karyotypic analysis; this sample did, however, have numerous genetic abnormalities identified by SNP-chip including hemizygous deletions of 3p25.1-p24.3 (2.29 Mb), 3p24.2-p24.1 (3.96 Mb), 3p23-q12.1 (66.55 Mb), 5q11.2-q-terminal (124.89 Mb), 7q11.23-q36.1 (76.04 Mb), 7q36.2 (0.78 Mb), 11q23.3-q-terminal (18.24 Mb), 17p-terminal-q11.1 (22.48 Mb), and 17q11.2-q12 (4.42 Mb); duplications of 3p24.3 (2.14 Mb), 5p15.31 (1.83 Mb), and 5p14.3-q11.2 (35.53 Mb); and trisomy of chromosomes 8, 21 and 22 (Table 2). To confirm these SNP-chip results, we performed extensive FISH analysis. The number of signals for probes D5S721 (5p15.2), D5S23 (5p15.2), D7Z1 (centromere of chromosome 7) and ABL (9q34.12) was two, and SNP-chip analysis also showed normal copy number (2n) consistent with the SNP-chip data. The EGR1 (5q31.2), D7S486 (7q31) and TP53 (17p13.1) probes revealed one signal; and these regions also showed hemizygous deletion (1n) by SNP-chip analysis. D8Z2 (centromere of chromosome 8), AML1 (21q22.12) and BCR (22q11.23) probes showed three or four signals, and SNP-chip analysis also indicated trisomy (3n) of these chromosomes. Chromosome 9 was normal by both SNP-chip and FISH analyses. As summarized in *Online Supplementary Table S3*, the results of SNP-chip and FISH analyses were completely congruent. Taken together, these results suggest that SNP-chip analysis reflected the genomic changes.

SNP-chip analysis in 37 normal karyotype acute myeloid leukemia/myelodysplastic syndrome samples

SNP-chip analysis of samples from 37 patients with normal karyotype AML/MDS revealed several genomic copy-number changes, as well as CNN-LOH. Nineteen patients (51%) had a normal genome by SNP-chip analysis (group A). In contrast, 18 patients (49%) had one or more genomic abnormalities (group B) (Figure 1). Deletions and/or duplications were found in nine patients (24%). Twelve patients (32%) had CNN-LOH. In group B, 14 cases (78% of the 18 samples) had only one genomic change; one case (6%) had two genomic abnormalities (case #5); two cases (11%) had three changes (case #2 and #4) and one case (5%) had four genomic alterations (case #20).

We also compared the relationship between the genomic changes and the French-American British classification of the 15 AML and 3 MDS samples in group B. In the AML samples, 11 cases had CNN-LOH, three cases had a duplication and seven cases had a deletion. The one AML M1 sample (case #10) had CNN-LOH; and the two AML M5b samples (cases #3 and #37) had CNN-LOH in their chromosomes. In the four AML M4 samples, cases #38, #21 and #2 had CNN-LOH, and cases #2 and #7 had a small deletion. In eight AML M2 samples, five (cases #4, #8, #17, #20, and #23) had CNN-LOH, three (cases #4, #5 and #20) had a duplication, and five (cases # 4, #5, #9, #20 and #26) had a deletion. In the three MDS samples, one sample (case #12) had CNN-LOH, and two samples (cases #13 and #41) had a deletion (Figure 1, Tables 3 and 4). Taken together, these results show that the patients who were categorized as having normal karyotype AML/MDS had easily recognizable deletions, duplications and/or CNN-LOH of their genome.

Table 2. **Copy-number changes in case #11 detected by SNP-chip analysis.**

Chromosome	Location	Physical localization: Proximal	Distal	Size (Mb)	Status
3	3p25.1-p24.3	16,389,202	18,675,075	2.29	Del
	3p24.3	19,589,378	21,731,557	2.14	Dup
	3p24.2-p24.1	24,881,910	28,844,599	3.96	Del
	3p23-q12.1	33,278,003	99,828,897	66.55	Del
5	5p15.31	7,616,335	9,443,217	1.83	Dup
	5p14.3-q11.2	18,603,838	54,129,781	35.53	Dup
	5q11.2-q-ter.	55,738,905	180,629,495	124.89	Del
7	7q11.23-q36.1	71,659,926	147,695,696	76.04	Del
	7q36.2	152,027,450	152,806,031	0.78	Del
8	Trisomy				
11	11q23.3-q-ter.	116,202,097	134,439,182	18.24	Del
17	17p-ter.-q11.1	18,901	22,494,871	22.48	Del
	17q11.2-q12	25,499,505	29,918,396	4.42	Del
21	Trisomy				
22	Trisomy				

AML case #11 had numerous genetic abnormalities. Location and size (Mb) were obtained from UCSC Genome Browser. Copy-number changes previously described as copy-number variant were excluded. Del: deletion; Dup: duplication; ter: terminal.

Chromosomal region and candidate genes in CNN-LOH detected by SNP-chip analysis

Previous studies demonstrated CNN-LOH in AML samples at a frequency of 15-20%.[11,30,50,51,53,54] Our analysis with AsCNAR (allele-specific copy-number analysis using anonymous references) revealed CNN-LOH in 32% of the AML/MDS samples with a normal karyotype; the median size of the CNN-LOH was 30.91 Mb (range, 11.76 Mb–103.77 Mb). We found some cases with a recurrent region of CNN-LOH. Cases #3 and #23 had CNN-LOH on 1p, and the common region of CNN-LOH (30.85 Mb) included the tyrosine kinase genes (*FGR*, *EPHA2* and *EPHB2*) and an imprinted tumor suppressor gene *TP73* (Table 3). Cases #2 and #38 had CNN-LOH on 6p and the common region of CNN-LOH (30.97 Mb) contained the tyrosine kinase gene *DDR1* (Table 3). Cases #4 and #37 had CNN-LOH on 8q and the common region of CNN-LOH (11.76 Mb) contained the tyrosine kinase gene *PTK* (Table 3). CNN-LOH of the

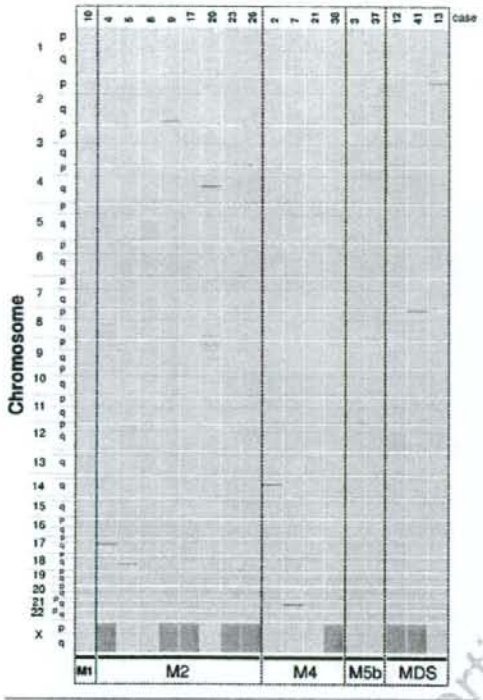

Figure 1. **Genomic DNA of 37 acute myeloid leukemia samples with normal karyotype were subjected to SNP-chip analysis; genomic abnormalities are summarized. Pink, green and red bars/boxes indicate CNN-LOH, deletion and duplication, respectively. Nineteen patients (51%) showed no detectable genomic abnormalities (*data not shown*), whereas 18 patients (49%) had one or more genomic abnormalities. Deletion or duplication was found in nine patients (24%), and CNN-LOH occurred in 12 patients (32%). Chromosomal location, size and genes are shown in Tables 3 and 4.**

whole region of 13q was found in cases #10 and #21; this region contains the *FLT3*, *FLT1*, *BRCA2* and *RB1* genes (Table 3).

Cases #2, #8, #12, #17 and #20 had CNN-LOH on 19p (13.41 Mb), 5q (103.77 Mb), 12q (96.23 Mb), 21q (29.54 Mb) and 9p (43.96 Mb), respectively. Although these regions of CNN-LOH occurred in only one case each, several interesting genes were found in the region, including *INSR*, *TYK2*, and *MATK* (case #2); *APC*, *FER*, *FMS/FLT4*, *PDGFRB*, *ITK* and *FGFR4* (case #8), *AML1/RUNX1* (case #17), and *JAK2* and *TEK* (case #20) (Table 3).

Interestingly, cases #10 and #21 had a *FLT3*-ITD gene mutation (Table 3); case #17 had an *AML1/RUNX1* frameshift caused by a deletion of cytosine at nucleotide 211 (Table 3). Sequencing of *JAK2* in case #20 showed a homozygous canonical *JAK2* mutation [V617F (GTC → TTC)] (Table 3). Each of these mutations occurred at a CNN-LOH. The data suggest that removal of a normal allele and duplication of the mutated allele is favored by the cancer cells.

Validation of copy number-neutral loss of heterozygosity

To validate CNN-LOH, we determined SNP sequences and gene-dosage in a CNN-LOH region using case #38 (Figure 2). If a chromosome has LOH, the nucleotide at the SNP site should not be heterozygous, but should be homozygous. We, therefore, examined six independent SNP sites in case #38 on the chromosome 6p region of CNN-LOH including rs7747259, rs1122637, rs9505293, rs6934027, rs280153 and rs191986. All six SNP sites showed only a single nucleotide; no SNP sites showed heterozygosity (Figure 2B). Each one of these sites is heterozygous in the general population at a frequency varying between 25% and 42% (*Entrez SNP database, http://www.ncbi.nlm.nih.gov/sites/entrez?db=snp*). These results strongly suggest that this region has LOH.

Next, we determined gene-dosage of the region to exclude the possibility of hemizygous deletion. The gene-dosage of 6p24.3 in case #38 was compared to that of normal genomic DNA using quantitative genomic real-time PCR by comparing the ratio between 6p24.3 and the reference genomic DNA, 2p21. As shown in Figure 2C, the amount of DNA at this site for case #38 was almost the same as that for normal genomic DNA, indicating that this region is not deleted. Taken together, our sequence data and gene dosage study validated the results of our SNP-chip analysis, clearly showing CNN-LOH at 6p24.3.

Chromosomal regions of copy-number change detected by SNP-chip analysis

Nine patients (24%) had small copy-number changes including deletions and/or duplications; the median size of the duplications and deletions was 0.3 Mb (range, 0.09–4.33 Mb) and 0.625 Mb (range, 0.11–5.87 Mb), respectively. As shown in Table 4, hemizygous deletions were found at 14q21.2 (0.3 Mb, case #2), 17q11.2 (2.7 Mb, case #4), 12p13.31 - p13.2 (2.91 Mb, case #5), 21q21.2 (0.44 Mb, case #7), 2q36.2 (0.41 Mb, case #9), 2p23.1 (0.56 Mb, case #13), 4q24 (1.08 Mb, case #20), 9p21.3 - p21.2 (5.87 Mb, case #20), 3p26.3 (0.69 Mb, case #26), and 8p23.2 (0.11 Mb, case #41). Cases #4, #5 and #20 had duplication at 1q43 (0.09 Mb), 18q21.2 (0.3 Mb), and 8q24.13 - q24.21 (4.33 Mb), respectively. These regions contain well-known oncogenes and tumor suppressor genes (Table 4). The tumor suppressor genes, *NF1* and *CDKN2A/CDKN2B*, and the transcription factor, *ETV6/TEL* were deleted in cases #4, #20 and #5, respectively; and the oncogene *MYC* was duplicated in case #20.

Validation of copy-number changes

Next, we validated copy-number changes in cases #20 and #5 using different techniques. Case #20 had duplication at 8q24.13 - q24.21 (Figure 3A) and hemizygous deletion at 9p21.3 - p21.2 (Figure 3B); these regions contain the oncogene *MYC* and the tumor suppressor genes *CDKN2A* and *CDKN2B*, respectively. Relative gene-dosages of the *MYC* and *CDKN2A* genes were examined by quantitative genomic real-time PCR with the chromosome 2p21 region as a control. The

level of the *MYC* gene was about 2-fold higher while the level of the *CDKN2A* gene was approximately 10-fold lower compared with normal genomic DNA (Figures 3C and D).

Chromosome 12p13.31 - p13.2 was deleted in case #5; this region contains the transcription factor *ETV6/TEL* (Figure 3E). FISH analysis with a probe of fluorescein-labeled ETV6-downstream (normal copy-number region) revealed two signals and a probe of Texas-red-labeled ETV6-upstream (hemizygous deleted region) revealed one signal (Figure 3F), validating the observations from SNP-chip analysis.

Table 3. **Chromosomal regions identified as CNN-LOH.**

Case*	FAB	Location	Physical localization Proximal	Distal	Size (Mb)	Genes
3	AML M5b	1p-ter.-p35.2	825,852	31,679,683	30.85	*FGR*
23	AML M2	1p-ter.-p35.1	825,852	33,526,200	32.7	*EPHA2, EPHB2 EPHA8, TPT3 LCK* (only #23)
2	AML M4	6p-ter. - p21.3	3119,769	31,094,483	30.97	*DDR1*
38	AML M4	6p-ter. - p21.3	1119,769	33,781,344	33.66	
4	AML M2	8q12.3 - q-ter.	64,069,382	146,106,670	82.04	*PTK2*
37	AML M5b	8q24.22 - q-ter.	134,507,898	146,263,538	11.76	*NBS1* (only #4)
10	AML M1	Whole 13q				*FLT3* (ITD)
21	AML M4	Whole 13q				*FLT1 BRCA2 RB1*
2	AML M4	19p-ter. - p13.13	212,033	13,625,099	13.41	*INSR, TYK2, MATK*
8	AML M2	5q13.3 - q-ter	76,761,338	180,536,297	103.77	*APC, FER, FMS/FLT4 PDGFRB, ITK, FGFR4, NPM1*
12	MDS RA	12q11 - q-ter.	36,144,018	132,377,151	96.23	*HER3*
17	AML M2	21q21.1 - q-ter.	17,346,621	46,885,639	29.54	*AML1/RUNX1* (delC211, frameshift)
20	AML M2	9p-ter. - p21.3 9p21.2 - q21.11	140,524 27,142,682	21,047,062 44,108,554	20.91 16.97	*JAK2* (V617F) *TEK*

*Twelve patients (32%) had CNN-LOH. Physical localization, size (Mb) and genes were obtained from UCSC Genome Browser. Note: Cases #10 and #21 had a mutant form of FLT3-internal tandem repeat (FLT3 (ITD)). Case #20 had a mutant JAK2 (JAK2 V617F) which is constitutively active, and case #17 had a deletion of cytosine at nucleotide 211 of AML1/RUNX1, resulting in a frameshift. * Known tyrosine kinase and tumor suppressor genes are shown.*

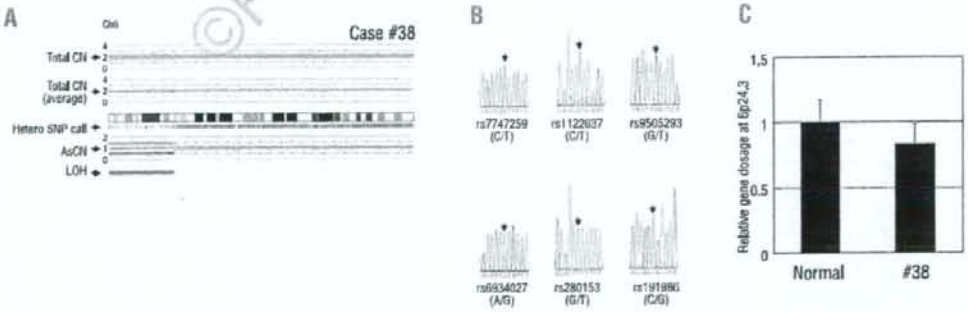

Figure 2. **Validation of CNN-LOH** (A) **Region of CNN-LOH in chromosome 6 of case #38. Red dots represent SNP sites as probes and indicate total copy-number. The blue line represents an average of copy-number and shows gene dosage. Green bars represents heterozygous (hetero) SNP calls. Red and green lines show allele-specific copy-number (AsCN). Blue bars indicate LOH detected by heterozygous SNP calls.** (B) **Determination of SNP sequences in the 6p region. Six independent SNP sites were sequenced. All six SNP sites contained only a single nucleotide; no SNP site displayed heterozygosity. Results are consistent with CNN-LOH.** (C) **Determination of gene-dosage in the 6p region. Gene-dosage of 6p24.3 (CNN-LOH region) in case #38 is compared to that in normal genomic DNA using quantitative genomic real-time PCR. Levels of the gene-dosage were determined as a ratio between 6p24.3 and the reference genomic DNA, 2p21.**

Table 4. **Chromosomal location of small copy-number changes.**

Cases	Type	Location	Physical localization Proximal	Physical localization Distal	Size (Mb)	Status	Gene*
4	AML M2	1q43	235,009,590	235,101,866	0.09	Dup	
		17q11.2	25,002,820	27,705,467	2.7	Del	*NF1*
5	AML M2	12p13.31-p13.2	9,312,096	12,218,922	2.91	Del	*ETV6/TEL*
		18q21.2	49,053,520	49,357,887	0.3	Dup	
9	AML M2	2q36.2	225,014,233	225,424,075	0.41	Del	
20	AML M2	4q24	105,640,274	106,723,813	1.08	Del	
		8q24.13 - q24.21	126,445,881	130,777,342	4.33	Dup	*MYC*
		9p21.3 - p21.2	21,063,692	26,935,976	5.87	Del	*CDKN2A, CDKN2B*
26	AML M2	3p26.3	1,221,075	1,911,873	0.69	Del	
2	AML M4	14q21.2	45,915,366	46,216,073	0.3	Del	
7	AML M4	21q21.2	23,126,095	23,566,855	0.44	Del	
41	MDS RA*	8p23.2	3,483,631	3,589,278	0.11	Del	
13	MDS RAEB-2	2p23.1	30,659,972	31,220,245	0.56	Del	

*Nine patients (24%) had deletion and/or duplication. Location, size (Mb), and genes were obtained from UCSC Genome Browser. Copy-number changes previously described as copy-number variant were excluded. Del: deletion. Dup: duplication. *Known oncogenes and tumor suppressor genes are shown.*

Relationship between genomic abnormalities and mutant genes within the region

In our normal karyotype AML/MDS samples, eight cases (21%) had *FLT3*-ITD and 14 cases (37%) had a *NPM1* mutation (Table 1). We compared genomic abnormalities, and *FLT3*-ITD and *NPM1* mutations (*Online Supplementary Table S4*). Both *FLT3*-ITD and *NPM1* were mutated in two samples in group A (11%) and four cases in group B (22%). A single mutation of *FLT3*-ITD was found in one sample in group A (5%) and one case in group B (6%); a single mutation of *NPM1* occurred in five samples in group A (26%) and three samples in group B (17%). These mutations were, therefore, dispersed between both groups A and B.

Relationship between genomic abnormalities and gene expression

We compared genomic abnormalities and gene expression. mRNA microarray analysis was done on all samples.[40] First, the level of mRNA expression in case #11 was compared with that in 37 normal karyotype AML samples. Affymetrix microarray analysis showed decreased average gene expression in the deleted regions and increased gene expression for regions with trisomy: the difference of average expression of genes located on deleted regions of chromosomes 5, 7, 17, as well as, trisomy 8, 21 and 22 were -0.21±0.01, -0.16 ±0.013, -0.27±0.018, +0.21±0.012, +0.22±0.022 and +0.15±0.013 (mean difference ± standard error), respectively (Figure 4A and *data not shown*).

Next, we examined the relationship between small copy-number changes and mRNA expression levels in the region. For this analysis, we chose deleted regions on chromosome 9 in case #20 (Figure 3B), chromosome 17 in case #4 (Table 4) and chromosome 12 in case #5 (Figure 3E). The differences in mean expression of genes located in deleted regions of chromosomes 9 (case #20), 17 (case #4), and 12 (case #5) were -0.15±0.07, -0.37±0.07, and -0.23±0.051 (mean difference ± standard error), respectively (Figure 4B). These results showed that large and small copy-number changes led to alterations of mRNA expression. In addition, the difference in mean expression of genes located in the CNN-LOH regions of each sample was comparable to that in normal copy-number samples, suggesting that CNN-LOH does not contribute to aberrant levels of gene expression (*data not shown*).

Discussion

Our genome-wide SNP-chip analysis of normal karyotype AML/MDS showed that 49% of these samples had one or more genomic abnormalities including deletions, duplications and CNN-LOH. Previous studies demonstrated that CNN-LOH occurs in AML samples at a frequency of 15-20%.[31,32,33,34,35,36] Of interest, about 40% of cases of relapsed of AML had CNN-LOH.[32] In our analysis, 32% of samples had CNN-LOH, and these regions of CNN-LOH contain several tyrosine kinase and tumor suppressor genes that may be candidate target genes in normal karyotype AML/MDS. In fact, the *FLT3*-ITD (13q12.2), *JAK2* V617F (9p24.1) and deletion of a cytosine at nucleotide 211 of *AML1/RUNX1* (21q22.12) occurred in areas of CNN-LOH resulting in duplication of these mutant genes and loss of the normal allele. A prior paradigm was that CNN-LOH marked the location of a mutated tumor suppressor gene, but it is clear that CNN-LOH can also be a signpost of an activated (mutated) oncogene. Of note, several CNN-LOH, including a region on chromosome 1p (cases #3 and #23), 6p (cases #2 and #38), 8q (cases #4 and 37) and 13q (cases #10 and #21), occurred in more than one sample. In addition, CNN-LOH of these regions, as well as several other unique CNN-LOH regions in our cohort, were also found in other stud-

ies.[30,31,35] Although these alterations are not frequent, shared regions of CNN-LOH clearly highlight their importance. These findings prompted us to screen genes located in CNN-LOH regions. We focused on tyrosine kinase genes including *FGR* (cases #3 and #23), *DDR1* (cases #2 and #38), *TYK2* (case #2), *MATK* (case #2), *FER* (case #8) and *FGFR4* (case #8), and either determined their exon nucleotide sequences or looked for single strand conformation polymorphism band-shifts of PCR products of the exons. However, these genes did not have detectable mutations (*data not shown*). Nevertheless, we believe that these CNN-LOH, as well as deletions and duplications, are acquired somatic mutations. We examined these regions for known copy-number polymorphisms (web site, *http://projects.tcag.ca/variation*) and found none. Also previously, we compared SNP-chip data between matched samples of acute promyelocytic leukemia and normal genomic DNA from the same individual (Akagi *et al.*, unpublished data) and found that CNN-LOH occurred only in the leukemia samples but not in the corresponding germline DNA. Furthermore, SNP-chip analysis easily detected a deletion on chromosome 3 (0.69 Mb) in case #28 in the AML sample which was not present in the remission bone marrow sample from the same individual (*Online Supplementary Figure S1*). Taken together, these findings suggest that the alterations detected by SNP-chip analysis are somatic mutations.

We also found small copy-number changes in some cases. Several features of case #20 are worthy of comment. The *MYC* gene was duplicated, and the *CDKN2A* (*p16/INK4A* and *p14/ARF*) and *CDKN2B* (*p15/INK4B*) genes were hemizygously deleted. Prominent expression of C-MYC protein is associated with stimulation of p14/ARF which inactivates MDM2, producing greater levels of p53 resulting in either apoptosis or slowing of cell growth which allows for DNA repair.[41,42] However, when the *p14/ARF* gene is deleted, C-MYC has an unfettered ability to stimulate growth of the cells. Case #20 had this constellation of changes. Furthermore, this individual had a homozygous *JAK2* mutation. *JAK2* is mutated (codon 617, valine changed to phenylalanine) and constitutively active in nearly 100%, 50% and 30% of samples from patients with polycythemia vera, agnogenic myeloid metaplasia and essential thrombocythemia, respectively, as well as in 1-3% of AML cases.[43-45] We do not know the prior history of this individual.

Some of the deleted genes are of particular interest; first, the tumor suppressor gene *NF1* was deleted in case #4. Children with neurofibromatosis type-1 have inactivating mutations of the *NF1* and an increased risk of developing juvenile myelomonocytic leukemia,[46] and LOH at the *NF1* gene locus occurs in this form of leukemia and other cancers. A recent study showed that three of 103 T-ALL (3%) samples and two of 71 AML samples with *MLL* rearrangements (3%) had deletion of the *NF1* gene region; a mutation in the remaining *NF1* allele was found in three samples, suggesting that *NF1* inactivation might be involved in the development of leukemia. Second, concerning case #5 (deletion of *ETV6/TEL*), *ETV6/TEL* is a transcriptional repressor and is involved in various translocations associated with

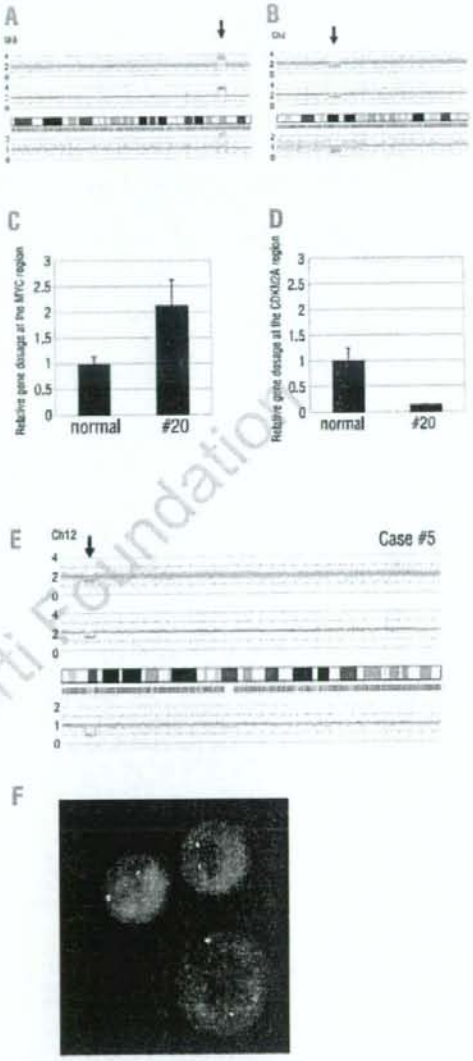

Figure 3. **Validation of duplication and deletion:** (A) **Chromosome 8q24.13-q24.21 is duplicated. This region contains the oncogene *MYC*.** (B) **Chromosome 9p21.3 - p21.2 shows a deletion. The deleted region contains the tumor suppressor genes *CDKN2A* (*p16/INK4A* and *p14/ARF*) and *CDKN2B* (*p15/INK4B*).** (C, D) **Gene-dosages of the *MYC* gene** (C) **and the *CDKN2A* gene** (D) **region in case #20 are compared to normal genomic DNA by quantitative genomic real-time PCR. Levels of the gene-dosage are determined as a ratio between target gene and the reference genomic DNA, 2p21.** (E) **Case #5 had hemizygous deletion in chromosome 12p13.31-p13.2; this region contains the transcription factor *ETV6/TEL* gene. Physical localization and size are presented in Table 4.** (F) **FISH analysis of case #5 with probes for the *ETV6/TEL* region. Probes of fluorescein-labeled ETV6-downstream (normal region by SNP-chip analysis) and Texas-red-labeled ETV6-upstream (hemizygous deleted region by SNP-chip analysis) revealed one and two signals, respectively.**

leukemia. About 30% of AML patients have loss of expression of the ETV6/TEL protein;[47,48] mutations of *ETV6/TEL* were found in 2% of AML samples, and these mutants behaved in a dominant-negative fashion.[48] Interestingly, previous array-comparative genome hybridization analysis of normal karyotype AML showed duplication of 8q24.13-q24.21 (including the *MYC* gene) and deletion of 12p12.3 (including the *ETV6* gene);[35] this constellation of alterations was also observed in our study.

Our microarray analysis showed that regions with copy-number loss or gain of chromosomal material

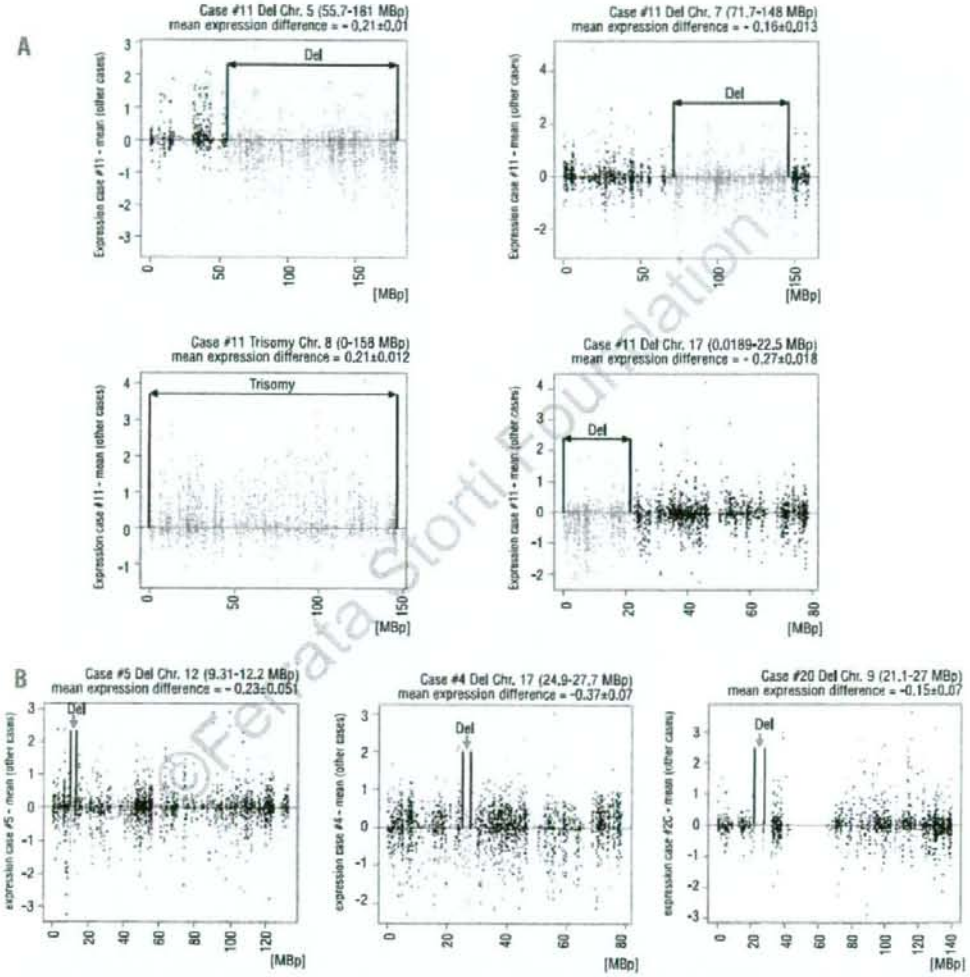

Figure 4. mRNA microarray analyses of acute myeloid leukemia samples. (A) Relationship between genomic abnormality and gene expression in acute myeloid leukemia case #11. mRNA microarray analysis was performed on all samples, and expression levels of acute myeloid leukemia cells from case #11 were compared to those of 37 normal karyotype acute myeloid leukemia samples. Affymetrix microarray analysis showed decreased average gene expression in the deleted regions, and increased average gene expression for trisomy 8: the difference of mean expression of genes located in the deleted region of chromosomes 5 (upper, left), 7 (upper, right), 17 (lower, right) and trisomy 8 (lower, left) were -0.21±0.01, -0.16±0.013, -0.27±0.018, and +0.21±0.012 (mean difference ± standard error), respectively. (B) Expression levels in acute myeloid leukemia cells from cases #20, #4 and #5 were compared with those in 36 normal karyotype AML samples. The differences in mean expression of genes located on the deleted region of chromosome 9 in case #20 (right), chromosome 17 in case #4 (middle), and chromosome 12 in case #5 (left) were -0.15±0.07, -0.37±0.07, and -0.23±0.051 (mean difference ± standard error), respectively. Each spot (black and red, Y-axis) indicates one gene and reflects the difference between each case and the mean of the other cases. Red spots represent genes located on an aberrant chromosome. The X-axis shows the chromosomal location.

were associated with either decreased or increased mRNA expression of genes in that same region, respectively, demonstrating the relationship between chromosomal status and gene expression. From an analysis perspective, we applied a descriptive approach and intended to assess plausibility of data. Some genes do indeed have higher expression values in deleted regions (Figure 4A, red points above zero) than in other cases, and some genes have lower values in trisomy (Figure 4A, red points below zero) than in other cases. However on average, expression in deleted regions is clearly lower than in non-deleted cases.

Because most regions are not recurring, we compared only one sample versus the rest (i.e. case #11 was compared with 37 normal karyotype AML/MDS cases; and cases #20, #4 and #5 were compared with other normal karyotype AML/MDS samples.) Various technical and biological sources of noise can confound the analysis. Overall, expression data appear to be consistent with chromosomal deletions and amplifications of the investigated regions. Further studies in larger cohorts of patients should enable prognostic stratification of patients in relation to their genomic changes and reveal new therapeutic targets.

Authorship and Disclosures

TA performed research, analyzed the data and wrote the paper; SO and MS performed SNP-chip analyses; GY and YN developed the CNAG; NK, AY, CWM and MD assisted in data analyses; SS, CH and TH provided AML samples, performed FISH analysis and aided in data analyses; HPK directed the overall study.

The authors declare no competing financial interests.

References

1. Kelly LM, Gilliland DG. Genetics of myeloid leukemias. Annu Rev Genomics Hum Genet 2002;3:179-98.
2. Estey E, Dohner H. Acute myeloid leukaemia. Lancet 2006;368:1894-907.
3. Erickson P, Gao J, Chang KS, Look T, Whisenant E, Raimondi S, et al. Identification of breakpoints in t(8;21) acute myelogenous leukemia and isolation of a fusion transcript, AML1/ETO, with similarity to Drosophila segmentation gene, runt. Blood 1992;80:1825-31.
4. Miyoshi H, Kozu T, Shimizu K, Enomoto K, Maseki N, Kaneko Y, et al. The t(8;21) translocation in acute myeloid leukemia results in production of an AML1-MTG8 fusion transcript. EMBO J 1993;12:2715-21.
5. Licht JD. AML1 and the AML1-ETO fusion protein in the pathogenesis of t(8;21) AML. Oncogene 2001;20:5660-79.
6. Peterson LF, Zhang DE. The 8;21 translocation in leukemogenesis. Oncogene 2004;23:4255-62.
7. Liu P, Tarlé SA, Hajra A, Claxton DF, Marlton P, Freedman M, et al. Fusion between transcription factor CBF beta/PEBP2 β and a myosin heavy chain in acute myeloid leukemia. Science 1993;261:1041-4.
8. Shigesada K, van de Sluis B, Liu PP. Mechanism of leukemogenesis by the inv(16) chimeric gene CBFB/PEBP2B-MHY11. Oncogene 2004;23:4297-307.
9. de Thé H, Chomienne C, Lanotte M, Degos L, Dejean A. The t(15;17) translocation of acute promyelocytic leukaemia fuses the retinoic acid receptor alpha gene to a novel transcribed locus. Nature 1990;347:558-61.
10. de Thé H, Lavau C, Marchio A, Chomienne C, Degos L, Dejean A. The PML-RAR-α fusion mRNA generated by the t(15;17) translocation in acute promyelocytic leukemia encodes a functionally altered RAR. Cell 1991;66:675-84.
11. Byrd JC, Mrózek K, Dodge RK, Carroll AJ, Edwards CG, Arthur DC, et al. Pretreatment cytogenetic abnormalities are predictive of induction success, cumulative incidence of relapse, and overall survival in adult patients with de novo acute myeloid leukemia: results from Cancer and Leukemia Group B (CALGB 8461). Blood 2002;100:4325-36.
12. Grimwade D, Walker H, Oliver F, Wheatley K, Harrison C, Harrison G, et al. The importance of diagnostic cytogenetics on outcome in AML: analysis of 1,612 patients entered into the MRC AML 10 trial. The Medical Research Council Adult and Children's Leukaemia Working Parties. Blood 1998;92:2322-33.
13. Mrozek K, Marcucci G, Paschka P, Whitman SP, Bloomfield CD. Clinical relevance of mutations and gene-expression changes in adult acute myeloid leukemia with normal cytogenetics: are we ready for a prognostically prioritized molecular classification? Blood 2007;109:431-48.
14. Caligiuri MA, Schichman SA, Strout MP, Mrózek K, Baer MR, Frankel SR, et al. Molecular rearrangement of the ALL-1 gene in acute myeloid leukemia without cytogenetic evidence of 11q23 chromosomal translocations. Cancer Res 1994;54:370-3.
15. Gilliland DG, Griffin JD. The roles of FLT3 in hematopoiesis and leukemia. Blood 2002;100:1532-42.
16. Reuter CW, Morgan MA, Bergmann L. Targeting the Ras signaling pathway: a rational, mechanism-based treatment for hematologic malignancies? Blood 2000;96:1655-69.
17. Pabst T, Mueller BU, Zhang P, Radomska HS, Narravula S, Schnittger S, et al. Dominant-negative mutations of CEBPA, encoding CCAAT/enhancer binding protein-alpha (C/EBPα), in acute myeloid leukemia. Nat Genet 2001;27:263-70.
18. Gombart AF, Hofmann WK, Kawano S, Takeuchi S, Krug U, Kwok SH, et al. Mutations in the gene encoding the transcription factor CCAAT/enhancer binding protein alpha in myelodysplastic syndromes and acute myeloid leukemias. Blood 2002;99:1332-40.
19. Falini B, Mecucci C, Tiacci E, Alcalay M, Rosati R, Pasqualucci L, et al. Cytoplasmic nucleophosmin in acute myelogenous leukemia with a normal karyotype. N Engl J Med 2005;352:254-66.
20. Falini B, Nicoletti I, Martelli MF, Mecucci C. Acute myeloid leukemia carrying cytoplasmic/mutated nucleophosmin (NPMc+ AML): biologic and clinical features. Blood 2007;109:874-85.
21. Nannya Y, Sanada M, Nakazaki K, Hosoya N, Wang L, Hangaishi A, et al. A robust algorithm for copy number detection using high-density oligonucleotide single nucleotide polymorphism genotyping arrays. Cancer Res 2005;65:6071-9.
22. Engle LJ, Simpson CL, Landers JE. Using high-throughput SNP technologies to study cancer. Oncogene 2006;25:1594-601.
23. Yamamoto G, Nannya Y, Kato M, Sanada M, Levine RL, Kawamata N, et al. Highly sensitive method for genomewide detection of allelic composition in nonpaired, primary tumor specimens by use of affymetrix single-nucleotide-polymorphism genotyping microarrays. Am J Hum Genet 2007;81:114-26.
24. Pfeifer D, Pantic M, Skatulla I, Rawluk J, Kreutz C, Martens UM, et al. Genome-wide analysis of DNA copy number changes and LOH in

CLL using high-density SNP arrays. Blood 2007;109:1202-10.
25. Lehmann S, Ogawa S, Raynaud SD, Sanada M, Nannya Y, Ticchioni M, et al. Molecular allelokaryotyping of early stage untreated chronic lymphocytic leukemia. Cancer 2008; 112:1296-305.
26. Mullighan CG, Goorha S, Radtke I, Miller CB, Coustan-Smith E, Dalton JD, et al. Genome-wide analysis of genetic alterations in acute lymphoblastic leukaemia. Nature 2007; 446:758-64.
27. Kawamata N, Ogawa S, Zimmermann M, Kato M, Sanada M, Hemminki K, et al. Molecular allelokaryotyping of pediatric acute lymphoblastic leukemias by high resolution single nucleotide polymorphism oligonucleotide genomic microarray. Blood 2008;111:776-84.
28. Flotho C, Steinemann D, Mullighan CG, Neale G, Mayer K, Kratz CP, et al. Genome-wide single-nucleotide polymorphism analysis in juvenile myelomonocytic leukemia identifies uniparental disomy surrounding the NF1 locus in cases associated with neurofibromatosis but not in cases with mutant RAS or PTPN11. Oncogene 2007;26:5816-21.
29. Fitzgibbon J, Iqbal S, Davies A, O'shea D, Carlotti E, Chaplin T, et al. Genome-wide detection of recurring sites of uniparental disomy in follicular and transformed follicular lymphoma. Leukemia 2007;21:1514-20.
30. Walker BA, Leone PE, Jenner MW, Li C, Gonzalez D, Johnson DC, et al. Integration of global SNP-based mapping and expression arrays reveals key regions, mechanisms, and genes important in the pathogenesis of multiple myeloma. Blood 2006;108:1733-43.
31. Raghavan M, Lillington DM, Skoulakis S, Debernardi S, Chaplin T, Foot NJ, et al. Genome-wide single nucleotide polymorphism analysis reveals frequent partial uniparental disomy due to somatic recombination in acute myeloid leukemias. Cancer Res 2005;65:375-8.
32. Fitzgibbon J, Smith LL, Raghavan M, Smith ML, Debernardi S, Skoulakis S, et al. Association between acquired uniparental disomy and homozygous gene mutation in acute myeloid leukemias. Cancer Res 2005;65:9152-4.
33. Tyybäkinoja A, Elonen E, Piippo K, Porkka K, Knuutila S. Oligonucleotide array-CGH reveals cryptic gene copy number alterations in karyotypically normal acute myeloid leukemia. Leukemia 2007;21:571-4.
34. Kiyoi H, Naoe T, Yokota S, Nakao M, Minami S, Kuriyama K, et al. Internal tandem duplication of FLT3 associated with leukocytosis in acute promyelocytic leukemia: Leukemia Study Group of the Ministry of Health and Welfare (Kohseisho). Leukemia 1997;11: 1447-52.
35. Schnittger S, Schoch C, Dugas M, Kern W, Staib P, Wuchter C, et al. Analysis of FLT3 length mutations in 1003 patients with acute myeloid leukemia: correlation to cytogenetics, FAB subtype, and prognosis in the AMLCG study and usefulness as a marker for the detection of minimal residual disease. Blood 2002; 100:59-66.
36. Schnittger S, Schoch C, Kern W, Mecucci C, Tschulik C, Martelli MF, et al. Nucleophosmin gene mutations are predictors of favorable prognosis in acute myelogenous leukemia with a normal karyotype. Blood 2005;106:3733-9.
37. Dicker F, Haferlach C, Kern W, Haferlach T, Schnittger S. Trisomy 13 is strongly associated with AML1/RUNX1 mutations and increased FLT3 expression in acute myeloid leukemia. Blood 2007;110: 1308-16.
38. Yin D, Xie D, Hofmann WK, Miller CW, Black KL, Koeffler HP. Methylation, expression, and mutation analysis of the cell cycle control genes in human brain tumors. Oncogene 2002;21:8372-8.
39. Bolstad BM, Irizarry RA, Astrand M, Speed TP. A comparison of normalization methods for high density oligonucleotide array data based on variance and bias. Bioinformatics 2003;19:185-93.
40. Haferlach T, Kohlmann A, Schnittger S, Dugas M, Hiddemann W, Kern W, et al. A global approach to the diagnosis of leukemia using gene expression profiling. Blood 2005;106:1189-98.
41. Hemann MT, Bric A, Teruya-Feldstein J, Herbst A, Nilsson JA, Cordon-Cardo C, et al. Evasion of the p53 tumour surveillance network by tumour-derived MYC mutants. Nature 2005;436:807-11.
42. Dang CV, O'Donnell KA, Juopperi T. The great MYC escape in tumorigenesis. Cancer Cell 2005;8:177-8.
43. Baxter EJ, Scott LM, Campbell PJ, East C, Fourouclas N, Swanton S, et al. Acquired mutation of the tyrosine kinase JAK2 in human myeloproliferative disorders. Lancet 2005; 365:1054-61.
44. Lee JW, Kim YG, Soung YH, Han KJ, Kim SY, Rhim HS, et al. The JAK2 V617F mutation in de novo acute myelogenous leukemias. Oncogene 2006;25:1434-6.
45. Illmer T, Schaich M, Ehninger G, Thiede C; DSIL2003 AML study group. Tyrosine kinase mutations of JAK2 are rare events in AML but influence prognosis of patients with CBF-leukemias. Haematologica 2007; 92:137-8.
46. Side LE, Emanuel PD, Taylor B, Franklin J, Thompson P, Castleberry RP, et al. Mutations of the NF1 gene in children with juvenile myelomonocytic leukemia without clinical evidence of neurofibromatosis, type 1. Blood 1998;92:267-72.
47. Hernández JM, González MB, García JL, Ferro MT, Gutiérrez NC, Marynen P, et al. Two cases of myeloid disorders and a t(8;12)(q12;p13). Haematologica 2000;85: 31-4.
48. Barjesteh van Waalwijk van Doorn-Khosrovani S, Spensberger D, de Knegt Y, Tang M, Löwenberg B, Delwel R. Somatic heterozygous mutations in ETV6 (TEL) and frequent absence of ETV6 protein in acute myeloid leukemia. Oncogene 2005;24:4129-37.
49. R Development Core Team. R: A language and environment for statistical computing. R Foundation for Statistical Computing, Vienna, Austria. 2007; ISBN 3-900051-07-0.
50. Serrano E, Camicer MJ, Orantes V, Estivill C, Lasa A, Brunet S, et al. Uniparental disomy may be associated with microsatellite instability in acute myeloid leukemia (AML) with a normal karyotype. Leuk Lymphoma 2008;49:1178-83.
51. Gupta M, Raghavan M, Gale RE, Chelala C, Allen C, Molloy G, et al. Novel regions of acquired uniparental disomy discovered in acute myeloid leukemia. Genes Chromosomes Cancer 2008;47:729-39.
52. Raghavan M, Smith LL, Lillington DM, Chaplin T, Kakkas I, Molloy G, et al. Segmental uniparental disomy is a commonly acquired genetic event in relapsed acute myeloid leukemia. Blood 2008;112:814-21.
53. Gorletta TA, Gasparini P, D'Elios MM, Trubia M, Pelicci PG, Di Fiore PP. Frequent loss of heterozygosity without loss of genetic material in acute myeloid leukemia with a normal karyotype. Genes Chromosomes Cancer 2005;44: 334-7.
54. Tyybäkinoja A, Elonen E, Vauhkonen H, Saarela J, Knuutila S. Single nucleotide polymorphism microarray analysis of karyotypically normal acute myeloid leukemia reveals frequent copy number neutral loss of heterozygosity. Haematologica 2008; 93:631-2.

ELSEVIER

Experimental Hematology

Experimental Hematology 2008;36:1471–1479

Genetic profiling of myeloproliferative disorders by single-nucleotide polymorphism oligonucleotide microarray

Norihiko Kawamata[a,*], Seishi Ogawa[b,*], Go Yamamoto[b], Soren Lehmann[a], Ross L. Levine[c], Yana Pikman[c], Yasuhito Nannya[b], Masashi Sanada[b], Carl W. Miller[a], D. Gary Gilliland[c], and H. Phillip Koeffler[a]

[a]*Hematology/Oncology, Cedars-Sinai Medical Center/UCLA School of Medicine, Los Angeles, Calif., USA;* [b]*Regeneration Medicine of Hematopoiesis, University of Tokyo, School of Medicine, Tokyo, Japan;* [c]*Hematology, Brigham and Women's Hospital, Harvard University, School of Medicine, Boston, Mass., USA*

(Received 10 January 2008; revised 11 June 2008; accepted 17 June 2008)

Objective. **Myeloproliferative disorders (MPD) are clonal hematopoietic diseases that include polycythemia vera (PV), essential thrombocytosis (ET), and primary myelofibrosis (PMF). Mutations in *JAK2* are present in many MPD patients. Additional genomic abnormalities are not fully examined in MPD.**

Materials and Methods. **We used single-nucleotide polymorphism DNA microarray (SNP-chip) to analyze 43 patients with MPD (10 PV, 17 ET, and 16 PMF) for genomic aberrations.**

Results. **Genomic abnormalities were rare in ET. The region containing either *RB* (13q14) or *NF1* (17q11) was deleted in 4 of the 16 PMF, especially PMF with no *JAK2* mutations. All five cases of PV having homozygous *JAK2*V617F had loss of heterozygosity with normal copy number [uniparental disomy] involving the gene. A subpopulation with 9p uniparental disomy was detected in 11 MPD (3 PV, 1 ET, 7 PMF). Uniparental disomy at 1p was found in one PV and three PMF. A novel mutation of *MPL* (Y591D), which was involved in this uniparental disomy, was found in 1 PV with *JAK2* mutation. The other three cases of PMF with 1p uniparental disomy had point mutations of the *MPL* gene, either a novel mutation (S204F) or the previously described W515L.**

Conclusion. **Genomic abnormalities, including 9p uniparental disomy/*JAK2* point mutations, 1p uniparental disomy/*MPL* point mutations, deletions of *RB1* and *NF1* are common alterations in MPD, especially in PMF.** © **2008 ISEH - Society for Hematology and Stem Cells. Published by Elsevier Inc.**

Myeloproliferative disorders (MPD) are clonal hematopoietic diseases that are classified based on their clinical features into subtypes that include polycythemia vera (PV), essential thrombocytosis (ET), and primary myelofibrosis (PMF) [1–3]. Recently, activating point mutations of *JAK2* kinase in exon 14 (V617F) [4–8] and exon 12 [9] have been detected in MPDs. These alterations transform JAK2 into a constitutively active kinase, leading to dysregulated proliferation of hematopoietic cells. *JAK2*V617F is detected in >90% of cases of PV and ~50% of cases of ET and PMF [4–8]. Further, a point mutation of the *MPL* gene (W515L) has been detected in PMF [10,11]. This point mutation also activates Jak2/Stat signal transduction and induces proliferation of hematopoietic cells and an MPD phenotype in murine models of disease [10].

Nevertheless, clonality analysis suggests that, at least in some cases, the *JAK2*V617F allele is acquired as a secondary event [12]. Thus, further genetic analysis is required to understand the pathophysiology of *JAK2*V617F-negative cases of ET and PMF, and to identify other acquired somatic mutations that contribute to disease pathogenesis in collaboration with *JAK2*V617F.

Recently, genomic microarray has been developed in which oligonucleotide probes corresponding to 50,000 to 1,000,000 chromosomal locations over the whole genome are placed on small glass plates. DNA extracted from cancer cells and normal cells are fragmented and labeled with fluorescence. The fluorescence-labeled DNA fragments are hybridized on the microarray, and the amount of DNA

*Drs. Kawamata and Ogawa contributed equally contributed to this work as the first authors.

Offprint requests to: Norihiko Kawamata, M.D., Hematology/Oncology, Cedars-Sinai Medical Center, UCLA School of Medicine, 8700 Beverly Boulevard, Los Angeles, CA 90048; E-mail: kawamatan@cshs.org

0301-472X/08 $–see front matter.
doi: 10.1016/j.exphem.2008.06.006

hybridized to each probe is measure on the scanner, leading to quantification of alleleic dosage at each genomic site. This technique allows detection of subcytogenetic deletions and amplification over the genome. Further, new screening platforms using arrayed oligonucleotide probes that contain single-nucleotide polymorphisms (SNP), so-called "SNP-chip," have been developed [13–15]. All probes on the SNP-chip are oligonucleotides containing SNPs and two types of probes (alleles A and B) are placed at each genomic locus. The probes are designed so that one nucleotide difference in two probes (alleles A and B) leads to different hybridization affinity of the probes. Therefore, SNP-chips are able to distinguish each parental allele (allele A or B) at heterozygous sites and to detect sensitively any alleleic imbalance at these sites [13–15]. Because probes on SNP-chips are designed based on reported SNP sequences, this technique cannot detect somatic mutations acquired in cancer cells. This technique allows detection of loss of heterozygosity with neutral allelic dosage [uniparental disomy] that cannot be identified by conventional methods, as well as, gain/loss of genomic materials at very high resolution [13–15]. We employed this technique for analysis of a set of *JAK2*V617F-positive (24 cases) or negative (19 cases) MPD samples to identify novel genomic abnormalities.

Materials and methods

Clinical samples and DNA preparation

Forty-three patients with MPD, including 10 PV (all *JAK2*V617F-positive); 17 ET, including 7 *JAK2*V617F–positive; and 10 *JAK2*V617F-negative cases and 16 PMF, including 10 *JAK2*V617F-negative and 6 *JAK2*V617F-positive cases were enrolled in this study after informed consents were obtained. DNA was extracted from neutrophils in the peripheral blood, using the standard proteinase K-phenol–chloroform extraction method. Bone marrow or peripheral blood cells were cultured in RPMI-1640 medium with 10% fetal bovine serum for 48 hours at 37°C. Chromosomes were G-banded using trypsin and Giemsa; karyotypes were described according to the International System for Human Cytogenetic Nomenclature.

SNP-chip analysis

SNP-chip of GeneChip Human mapping 50 k array XbaI 240 was used for this study (Affymetrix, Tokyo, Japan). Fragmentation and labeling of DNAs were performed using GeneChip resequencing kit (Affymetrix) according to manufacturer's protocols. Hybridization, washing, and signal detection were performed on a GeneChip Fluidics Station 400 and GeneChip scanner 3000 according to manufacturer's protocols (Affymetrix).

To reduce noise, we used "local mean analysis" as described previously [16]. In brief, the sequence of the mean log 2 ratios,

$$ {}^{c}\overline{A}^{test,\,REF}_{i,k} = 1/k \sum_{i}^{i+k-1} {}^{c}A^{test,\,REF}_{i} $$

is calculated where k is the number of terms to be averaged and arbitrarily set from 3 to 10, according to the SD values after compensations of log 2 ratios and optimization of non-references for diploid SNPs. In the alternative analysis using a hidden Markov model, the inference of copy number is more efficient and automated, in which a real state of the copy number sequence (a hidden state) along a chromosome is inferred from the observed sequence ${}^{c}A^{test,\,REF}_{i}$ as the state of maximum likelihood that is calculated from the state transition load and the probability of the hidden state to "emit" the observed sequence of log 2 ratios, using the Viterbi algorithm [16]. We assumed that copy number change is the result of a genetic recombination event between the two adjacent SNP loci, and Kosambi's map function $(1/2)\tanh(2\theta)$ is used to transform the genomic distance, or recombination fraction between the two SNPs (θ) to state "transition probability," where θ is expressed in cM units; for simplicity, 1 cM should be 1 Mbp. The observed log 2 ratio is assumed to follow the normal distribution according to real copy number states, which gives the "emission probability." The variables of normal distribution were empirically determined from the experimental data [16].

Allele-specific PCR for JAK2 mutation

Allele-specific polymerase chain reaction (PCR) was performed according to the method previously reported to detect *JAK2* V617F mutations [4]. All 43 MPD cases were examined using mutation-specific primers and wild-type–specific primers for the *JAK2* gene as reported previously [4]. All PCR products were electrophoresed in 2% agarose gels containing ethidium bromide. PCR bands were visualized under ultraviolet light and photographed.

Quantitative genomic PCR

Quantitative genomic PCR was performed using real-time PCR technique as described previously. Gene dosage of the *NF1* and *RB* was measured [14]. All primers used for the quantitative genomic PCR are listed in Supplementary Table 1.

PCR and sequencing

All coding exons of *FGR1*, *TIE1*, and *MPL* genes were amplified from selected samples using the PCR technique. The primers used for amplification of the *MPL* gene are listed in the Supplementary Table 1. The PCR conditions were as follows: 40 cycles of 94°C, 30 seconds for denaturing, 55°C, 30 seconds for annealing, and 73°C, 30 seconds for extension. All PCR products were electrophoresed in a 2% agarose gel; PCR bands were excised, and purified using Qiagen Gel extraction kit (Qiagen, Valencia, CA, USA) according to manufacturer's protocols. Purified PCR bands were directly sequenced using the Big-dye sequence reaction (Applied Biosystems, Foster City, CA, USA) and analyzed on an Autosequencer 3100 (Applied Biosystems). PCR products which had mutations of S204F-*MPL* (*MPL* exon 4), W515L (*MPL* exon 10), Y591D (*MPL* exon 12) as detected by direct sequencing were cloned into pGEM-T vectors (Promega) and transformed into *Escherichia coli*–competent cells. Plasmids were extracted from eight independent clones of each PCR product and their nucleotide sequences were determined.

Screening of normal DNA

DNA from 100 normal volunteers and 42 MPD patients were screened for S204F and Y591D mutations of the *MPL* gene.

PCR products of exon 4 of *MPL* were digested with AlwNI for the S204F mutation (wild-type is digested and mutant is not digested); PCR products of exon 12 of *MPL* were digested with BsiEI for the Y591D mutation (wild-type is not digested and mutant is digested). The treated PCR products were run in 2% agarose gel.

Expression of MPL in BaF/3 cells

Human full-length *MPL* cDNA was cloned into pMSCV vector (Clontech, Mountain View, CA, USA) from normal human bone marrow cells using PCR. EGFP cDNA (Clontech) was ligated into the pMSCV vector as a marker protein driven by the pGK promoter. S204F, W515L, and Y591D mutations were introduced into pMSCV-EGFP-hMPL vector by the PCR mutagenesis method. Expression of wild-type and mutant MPL was driven by LTR. The constructs were electroporated into the murine interleukin-3 (IL-3)–dependent B-cell line, BaF/3, and cultured in media containing IL-3 for 2 days. Green fluorescent protein–positive cells were selected by fluorescein-activated cell sorting and cultured in media without IL-3. Cell numbers were counted on days 2, 4, and 6.

Results

Chromosomal duplications and deletions in MPDs

Genetic abnormalities, including deletions and duplications, are shown in Figures 1A to C and summarized in Table 1. Gain of genomic materials was detected in 5 of the 43 MPD samples; loss of genomic materials was detected in 9 of 43 MPD cases. Trisomy 9 was detected in one PV and one ET; duplication of 9 p was identified in one PV; duplication of 9q21.11-qter was detected in one PMF.

Seven of 16 samples of PMF had loss and/or gain of genomic material. Notably, five of the nine cases of PMF with no *JAK2* mutations had genomic alterations, including deletion involving *RB1* (13q14) (PMF case nos. 29, 84, and 287); deletion involving *NF1* (17q11) (PMF case no. 485), duplication of 8q21.3, duplication of 9q21.11-qter, duplication of 4q28.1-qter, deletion of 12p13 and deletion of 4q24. Deletion of 4q24 (PMF case no. 109) was also detected by conventional cytogenetics confirming the SNP-chip results (data not shown). Deletions of *NF1* and *RB1* were also confirmed by quantitative genomic PCR (Suppl. Fig. 1).

Only 2 of 17 ET cases had genomic alterations; those with wild-type *JAK2* (10 cases) had a normal genomic pattern (Table 1). One case of ET had deletion at 5q23.1 involving a single gene, LOC51334. We analyzed nucleotide sequences of all exons of the remaining allele, as well as, methylation status of the promoter region of this gene in this case; and found neither methylation nor mutation of the gene (data not shown).

9p uniparental disomy and JAK2 point mutations in MPD

One of the advantages of SNP-chip analysis is the ability to detect uniparental disomy [17]. This novel analysis can detect uniparental disomy even when clones with uniparental disomy are not dominant [17]. We found uniparental disomy in the 9 p region that involved *JAK2* in five PV samples, in which the clones with the uniparental disomy were dominant (Fig. 2A and Table 1) because large regions of loss of heterozygosity without loss of DNA copy number were detected. Each of these cases showed homozygous *JAK2*V617F mutations by allele specific PCR (Table 1).

Further, we identified 11 cases with 9 p uniparental disomy (3 PV, 1 ET, and 7 PMF), in which these clones were not dominant (Table 1). Although regions with loss of heterozygosity of 9 p in these cases were quite obvious, allele-specific gene-dosage analysis clearly indicated that dosage level of one of the parental alleles was lower than normal level, and the other parental allele was higher (Fig. 2B).

One PV and one ET had both wild-type *JAK2* and *JAK2*V617F with trisomy 9. Another PV had both wild-type *JAK2* and *JAK2*V617F with duplication of 9 p, but we were unable to determine if either the mutant or wild-type allele was duplicated in these cases.

Point mutations of the MPL gene in MPD with 1p uniparental disomy

SNP-chip analysis showed 1 p uniparental disomy in two cases of PMF (case nos. 29 and 84) (Fig. 3A), suggesting the possibility of a transforming allele in this region. Analysis of the common region of uniparental disomy on 1 p of these two cases of PMF showed two tyrosine kinase (*FGR* and *TIE1*) genes and the thrombopoietin receptor (*MPL*) gene; each is known to be expressed in normal hematopoietic cells [18–20]. We sequenced all coding exons of the *FGR*, *TIE1*, and *MPL* genes in these two PMF cases. No mutations in the *FGR* and *TIE1* genes were detected (data not shown). However, we found a point mutation in the *MPL* gene that changed codon 204 from TCT to TTT (S204F) in case no. 29 (Fig. 3B) and changed codon 515 from TGG to TTG (W515L) in case no. 84 (Fig. 3C). Each sample had no wild-type allele as shown by direct sequencing analysis (Figs. 3B and C).

In another sample of PMF (case no. 325) and PV (case no. 298), 1 p uniparental disomy was detected in a subpopulation of the tumor cells (Fig. 4). We sequenced all exons of the *MPL* gene in these two cases and found point mutations of the *MPL* gene (W515L and Y591D) (Fig. 4). In case no. 325 of PMF, TGG changed to TTG at amino-acid 515, leading to substitution of leucine for tryptophan (Fig. 4A); in case no. 298 of PV, TAC changed to GAC at amino-acid position 591, leading to substitution of aspartic acid for tyrosine (Fig. 4B). In these cases, wild-type sequences were detected as well, suggesting that clones with these mutations were not predominant. All point mutations were also confirmed after subcloning of the PCR products into plasmids (data not shown). Positions of the *MPL* mutations are shown in Figure 5; S204F mutation is in the extracellular region; W515L and Y591D are in the cytoplasmic domain.

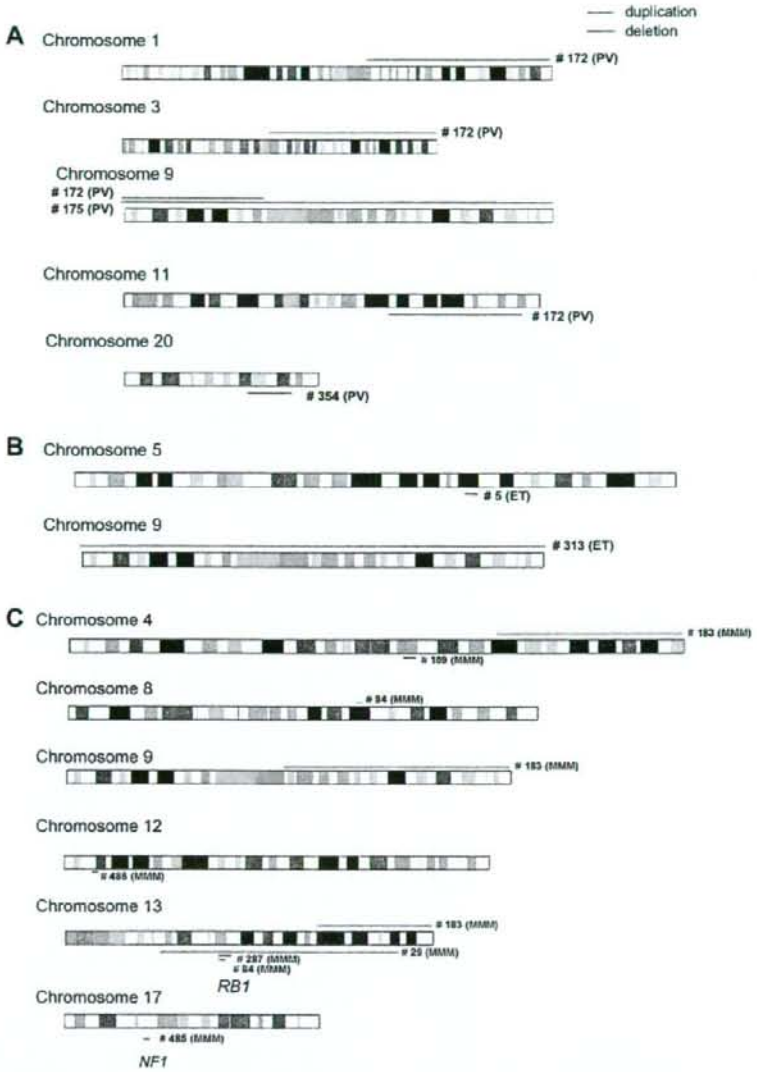

Figure 1. Chromosomal duplications and deletions in myeloproliferative disorder samples as detected by single-nucleotide polymorphism DNA microarray (SNP-chip). Duplications are indicated as red lines above the chromosomes; deletions are displayed as blue lines under the chromosomes. Case numbers are shown to the right of the chromosomes. Results of polycythemia vera (PV) (**A**), essential thrombocytosis (ET) (**B**), and myelofibrosis with myeloid metaplasia (**C**) are shown. PMF = primary myelofibrosis.

Discussion

Recently, we developed a new algorithm for SNP-chip analysis that reduced noise (false-positive and false-negative results), making the data more reliable [16,17]. We have previously validated the sensitivity and specificity of the SNP-chip analysis using genomic real time PCR, fluorescence in situ hybridization, and nucleotide sequencing [14–17]. This platform and our novel algorithm allow detection of very small genomic abnormalities at a very high sensitivity [14–17].

Comparison between tumor samples and matched control samples is the best way to detect genomic loss/gain in cancer samples. However, it is not always possible to obtain matched control samples. As reported by a number of

Table 1. Genomic abnormalities detected by SNP-Chip in MPDs

Disease	case #	JAK2	UPD	UPD*	Recurrent	Other abnormalities	MPL**
PV	78	1		9p		dup 9p, dup 3q, Trisomy 4, del 11q	
	172	1				Trisomy 9	
	175	1					
	298	1		1p/9p			Y591D
	375	1		9p			
	86	2	9p				
	249	2	9p				
	307	2	9p				
	327	2	9p				
	354	2	9p			Del 20q	
ET	114	0					
	115	0					
	146	0					
	201	0					
	240	0					
	281	0					
	285	0					
	314	0					
	446	0					
	461	0					
	5	1				Del 5q23.1(LOC51334)	
	186	1					
	271	1					
	272	1					
	313	1				Trisomy 9	
	330	1		9p			
	374	1					
MMM	29	0	1p		RB del		S204F
	56	0					
	84	0	1p		RB del	Dup 8q21.3	W515L
	138	0					
	183	0				Dup 9q21.11-qter, Dup 4q28.1-qter	
	196	0					
	325	0		1p			W515L
	459	0					
	485	0			NF1 del	Del 12p13	
	109	1		9p		Del 4q24	
	120	1		9p			
	122	1		9p			
	191	1		9p			
	287	1		9p	RB del		
	442	1		9p			
	457	1		9p			

UPD: uniparental disomy, Del: deletion, Dup: duplication.
JAK2: Mutational status of JAK2 gene; 0, only wild-type JAK2 allele was detected;
1, both wild-type and mutated alleles of JAK2 were detected;
2, only mutated allele of JAK2 was detected.
*: Subpopulation had UPD which was detected by allele-specific gene dosage analysis.
**: Mutational status of MPL gene (see Result Section)

investigators, the human genome has copy number variants (CNV), and many genomic sites of CNV have been reported [21–24]. When allelic copy numbers of tumor samples are compared with nonmatched control samples, differences of copy numbers at CNV sites could be interpreted as either a deletion or amplification/duplication. However, these are not pathological abnormalities, but caused by variants. In our study, we used non–self-reference data for comparison. We excluded the known regions of CNV in our study, therefore, the abnormalities found here are unlikely to be areas of CNV.

SNP-chip is a powerful tool for genome-wide analysis of genetic abnormalities [14,15]. It allows for detection of small deletions and amplification that cannot be detected by standard karyotyping techniques [14,15]. Using this approach, commonly deleted and/or amplified regions of the genome can be defined to facilitate the identification of target tumor suppressor genes and/or oncogenes in these

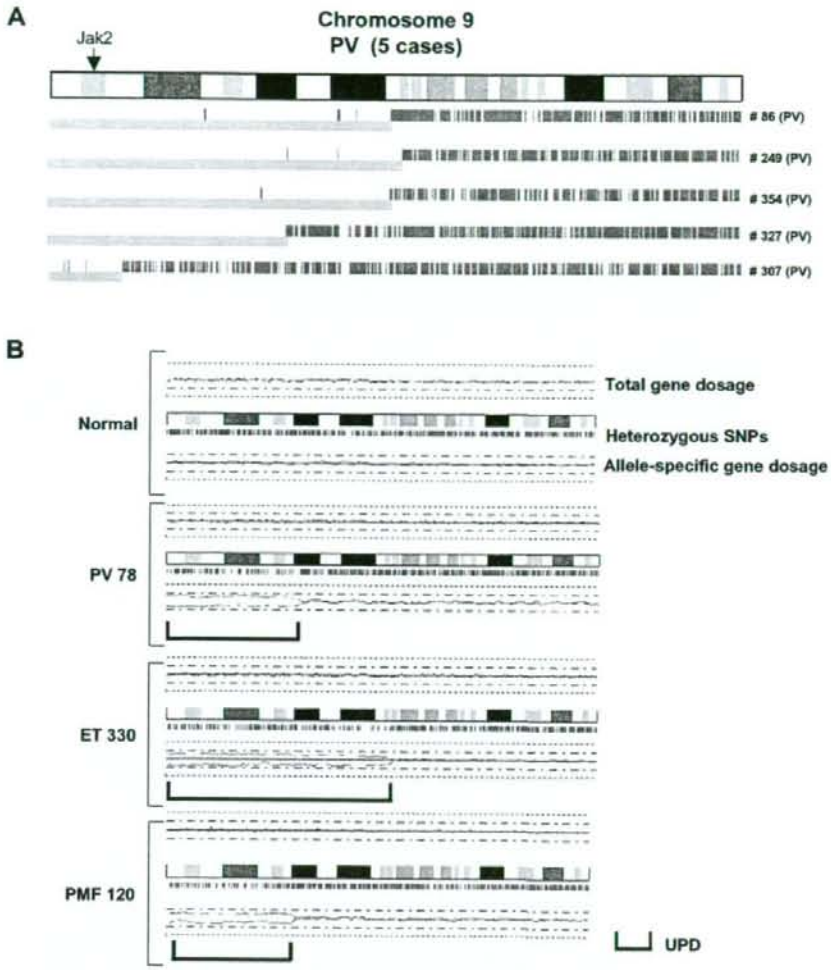

Figure 2. Uniparental disomy of 9 p in myeloproliferative disorder samples. (**A**) Uniparental disomy in dominant clones. Green bars indicate heterozygous single-nucleotide polymorphism (SNPs). Regions with pink lines show those regions with loss of heterozygosity but with normal DNA copy number (uniparental disomy). Position of *JAK2* gene is indicated by an arrow. Case numbers are shown to the right of the chromosomes. (**B**) Uniparental disomy in nondominant clone. Representative cases having nondominant clones with 9 p uniparental disomy are shown. In each panel, a blue line at the top indicates level of total gene dosage. Green bars under the chromosome indicate heterozygous SNP sites detected by SNP-chip analysis. Green and red lines in the bottom in each panel demonstrate levels of parental gene dosage. Uniparental disomy regions have decrease of one of the parental gene dosage (green line) and increase of gene dosage of the other parental allele (red line). ET = essential thrombocytosis; PMF = primary myelofibrosis; PV = polycythemia vera; UPD = uniparental disomy.

loci. For example, we identified deleted regions of PMF that include either the *RB1* (13q14) or *NF1* (17q11) locus.

Recently, uniparental disomy that is not detectable by conventional techniques has been reported in human cancers [14,25,26]. Most investigators have assayed for loss of heterozygosity using microsatellite markers, combined with fluorescence in situ hybridization to detect uniparental disomy [26]. A region was defined as having uniparental disomy when fluorescence in situ hybridization displayed an intact chromosome pattern and the loss of heterozygosity analysis demonstrated allelic imbalance at the locus [26]. However, this approach is both time- and labor-intensive compared with use of SNP-chip for detection of uniparental disomy. For example, we detected five PV cases with 9 p uniparental disomy. Each 9 p uniparental disomy case had two *JAK2* mutated

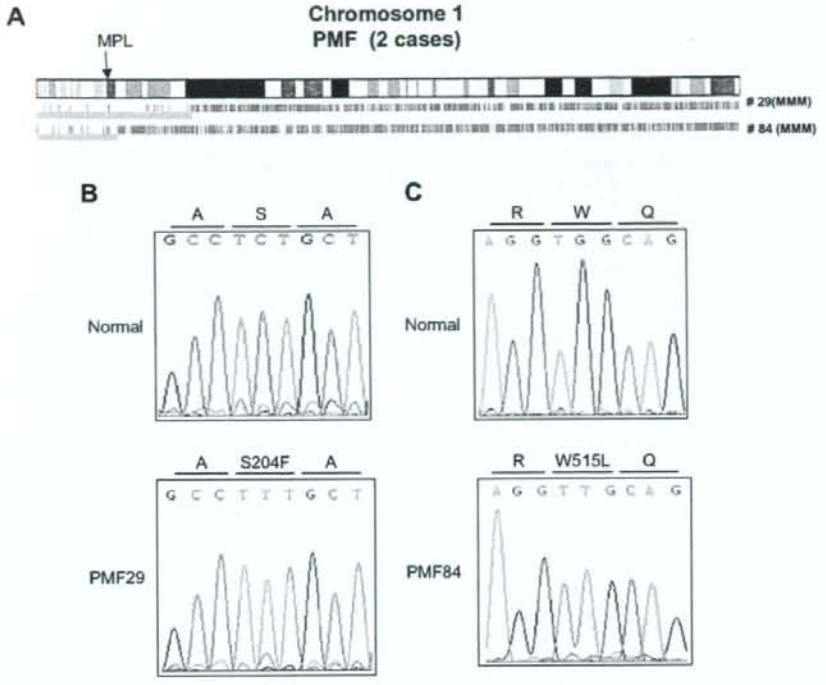

Figure 3. Uniparental disomy of 1 p and point mutations of *MPL* in primary myelofibrosis (PMF). (**A**) Two cases of PMF with clear uniparental disomy in the 1 p region are shown. Green bars indicate heterozygous single-nucleotide polymorphism (SNPs). Regions with pink lines show those regions with loss of heterozygosity but with normal DNA copy number (uniparental disomy). Position of *MPL* gene is indicated by an arrow. Point mutations of *MPL* found in two PMF cases are shown: S204F (**B**) and W515L (**C**). The sequences were determined by direct nucleotide sequencing. Sequences of normal alleles are shown in the upper panels. UPD = uniparental disomy.

alleles as confirmed by allele-specific PCR. As previously reported, uniparental disomy is a common mechanism for duplication of the mutant *JAK2*V617F allele in PV [6], presumably through mitotic recombination and subsequent positive selection for clones harboring two mutant alleles. We previously developed a new algorithm allowing us to evaluate allele-specific gene dosage (gene dosages of paternal and maternal alleles) without matched control samples [17]. This new algorithm can very sensitively and accurately detect uniparental disomy regions even though the clones with uniparental disomy are as small as 20% of whole tissues [17]. We previously found that 9 p uniparental disomy in nondominant clones were frequent events in MPD [17].

Using this method, we could detect nondominant clones with 9 p and/or 1 p uniparental disomy, which may be overlooked by standard algorithm used for SNP-chip analysis. Uniparental disomy was a very frequent event in PMF; three cases had 1 p uniparental disomy and seven cases had 9 p uniparental disomy. In contrast, only one of the ET cases in this study had uniparental disomy. In ET, we only found one sample with deletion of 5q23.1 and another with trisomy 9, as well as, 7 cases with a *JAK2* mutation. This observation could be explained by either lack of involvement of the granulocytic lineage (our source of DNA) in these ET patients, or by point mutations or other genetic abnormalities in these samples that were not detected by SNP-chip analysis. Clearly, the pathogenesis leading to ET, especially ET without a *JAK2* mutation, remains to be elucidated.

We detected a novel 1 p uniparental disomy in samples from three PMF and one PV individuals. Because chromosomal regions of uniparental disomy are hotspots of genes mutated in cancers, we screened all coding exons of several candidate genes, including *MPL*, in the 1 p region by direct nucleotide sequencing. In each case, we found a point mutation of the *MPL* gene; two samples involved the well-know mutation, W515L [10,11], and the other two were novel mutations (S204F and Y591D). Unfortunately, because the matched control samples of these cases were not available, we could not examined if these changes were found in their germline. Nevertheless, we did screen 100 DNA samples from normal individuals to determine if the nucleotide substitutions (S204F and Y591D) were polymorphic; we did not

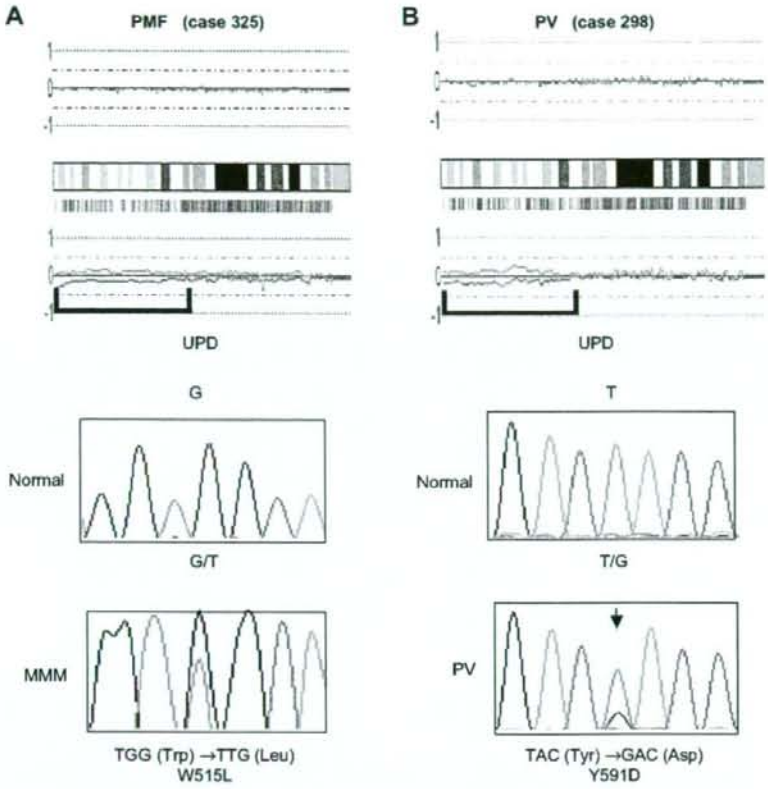

Figure 4. Nondominant clones with 1 p uniparental disomy in myeloproliferative disorder were detected by single-nucleotide polymorphism DNA microarray (SNP-chip). Top panels: Allele-specific gene dosage analysis. Blue lines above the chromosomal panels indicate levels of total gene dosage (0 indicates 2 N, normal diploid). Green and red lines below the chromosomal panels indicate respective parental allele gene dosage. Higher level of the red line and lower level of the green line indicates the regions of uniparental disomy. Middle and bottom panels: normal (middle) and mutated (bottom) nucleotide sequences of the *MPL* gene encoding amino-acid positions at 515 and 591; primary myelofibrosis (PMF) case 325 (**A**) had W515L mutation and polycythemia vera (PV) case 298 (**B**) had Y591D mutation. UPD = uniparental disomy.

detect these nucleotide substitutions in normal DNA (data not shown). We screened all of our remaining MPD cases for these mutations (S204F, W515L, and Y591D) and found none (data not shown). Amino-acid substitution of MPL was found in all cases with 1 p uniparental disomy, suggesting that these substitutions are mutations, not rare polymorphisms, and MPL gene is a target gene of 1 p uniparental disomy. 1 p uniparental disomy may be a hallmark for a *MPL* mutation in MPD. The precise function of novel MPL mutants (S204F and Y591) remains to be explored.

To elucidated functional significance of these novel mutations of the *MPL* gene, we expressed them in the IL3-dependent murine B-cell line, BaF/3 cells. Mutant S204F or Y591D MPL did not allow the cells to grow independently of IL-3, whereas W515L MPL did (data not shown). Unfortunately, because the peripheral blood and/or bone marrow cells from these patients were not available, we were not able to examine bone marrow hematopoietic stem cells for these abnormalities. How these novel MPL mutants contribute to development of PMF is unclear. Interestingly, one PV (case 298) had a point mutation of both a *JAK2* and *MPL* (Y591D), suggesting that mutations

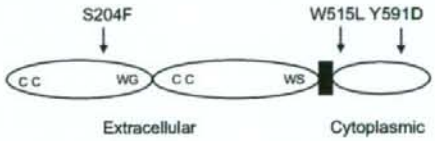

Figure 5. Position of point mutations of the *MPL* gene found in myeloproliferative disorder. Schema of the MPL protein. Position of the point mutations are indicated by arrows. CC = conserved cysteine residues; WG = WGXWS motif; WS = WSXWS motif; extracellular: extracellular domain; cytoplasmic: cytoplasmic domain; black box depicts the transmembrane domain.

of these two molecules may independently contribute to development of MPD, even though they are involved in the same Mpl/Jak/Stat signal transduction pathway.

Myelofibrosis, not thrombocytosis, is a prominent feature in PMF [1]. How an activating point mutation of *MPL* by itself can induce myelofibrosis is unclear. Interestingly, two cases with *MPL* mutations had deletion of the *RB1* gene. Mutation of *MPL* and deletion of *RB1*, may cooperate in development of PMF; or loss of *RB1* may potentiate acquisition of mutations of *MPL*.

In summary, we found recurrent genetic abnormalities, including 9 p uniparental disomy/*JAK2* mutations, 1 p uniparental disomy/*MPL* mutations, as well as deletions of the *RB* and the *NF1* genes in MPD. We found two novel point mutations of the *MPL* gene (S204F and Y591D) in PMF and PV samples with 1 p uniparental disomy. Genomic abnormalities, including point mutations, deletions, and uniparental disomy may cooperate in development of MPD. In regions of deletions, duplications/amplifications, and uniparental disomy, critical target genes may be altered. Accumulation of data of SNP-chip analysis will narrow the common abnormal genomic regions and help to clone novel mutated genes in MPD. SNP-chip analysis is a robust tool to detect genetic abnormalities, especially small deletions and uniparental disomy in MPD.

References

1. Tefferi A. Myelofibrosis with myeloid metaplasia. N Engl J Med. 2000;342:1255–1265.
2. Spivak JL. Diagnosis of the myeloproliferative disorders: resolving phenotypic mimicry. Semin Hematol. 2003;40(Suppl 1):1–5.
3. Thiele J, Kvasnicka HM, Orazi A. Bone marrow histopathology in myeloproliferative disorders—current diagnostic approach. Semin Hematol. 2005;42:184–195.
4. Baxter EJ, Scott LM, Campbell PJ, et al. Acquired mutation of the tyrosine kinase JAK2 in human myeloproliferative disorders. Lancet. 2005;365:1054–1061.
5. James C, Ugo V, Le Couedic JP, et al. A unique clonal JAK2 mutation leading to constitutive signalling causes polycythaemia vera. Nature. 2005;434:1144–1148.
6. Kralovics R, Passamonti F, Buser AS, et al. A gain-of-function mutation of JAK2 in myeloproliferative disorders. N Engl J Med. 2005;352:1779–1790.
7. Levine RL, Wadleigh M, Cools J, et al. Activating mutation in the tyrosine kinase JAK2 in polycythemia vera, essential thrombocythemia, and myeloid metaplasia with myelofibrosis. Cancer Cell. 2005;7:387–397.
8. Zhao R, Xing S, Li Z, et al. Identification of an acquired JAK2 mutation in polycythemia vera. J Biol Chem.. 2005;280:22788–22792.
9. Scott LM, Tong W, Levine RL, et al. JAK2 exon 12 mutations in polycythemia vera and idiopathic erythrocytosis. N Engl J Med. 2007;356:459–468.
10. Pikman Y, Lee BH, Mercher T, et al. MPLW515L is a novel somatic activating mutation in myelofibrosis with myeloid metaplasia. PLoS Med. 2006;3:e270.
11. Pardanani AD, Levine RL, Lasho T, et al. MPL515 mutations in myeloproliferative and other myeloid disorders: a study of 1182 patients. Blood. 2006;108:3472–3476.
12. Levine RL, Belisle C, Wadleigh M, et al. X-inactivation-based clonality analysis and quantitative JAK2V617F assessment reveal a strong association between clonality and JAK2V617F in PV but not ET/MMM, and identifies a subset of JAK2V617F-negative ET and MMM patients with clonal hematopoiesis. Blood. 2006;107:4139–4141.
13. Garraway LA, Widlund HR, Rubin MA, et al. Integrative genomic analyses identify MITF as a lineage survival oncogene amplified in malignant melanoma. Nature. 2005;436:117–122.
14. Kawamata N, Ogawa S, Zimmermann M, et al. Molecular allelokaryotyping of pediatric acute lymphoblastic leukemias by high resolution single nucleotide polymorphism oligonucleotide genomic microarray. Blood. 2008;111:776–784.
15. Lehmann S, Ogawa S, Raynaud SD, et al. Molecular allelokaryotyping of early stage untreated chronic lymphocytic leukemia. Cancer. 2008;112:1296–1305.
16. Nannya Y, Sanada M, Nakazaki K, et al. A robust algorithm for copy number detection using high-density oligonucleotide single nucleotide polymorphism genotyping arrays. Cancer Res. 2005;65:6071–6079.
17. Yamamoto G, Nannya Y, Kato M, et al. Highly sensitive method for genomewide detection of allelic composition in nonpaired, primary tumor specimens by use of affymetrix single-nucleotide-polymorphism genotyping microarrays. Am J Hum Genet. 2007;81:114–126.
18. Batard P, Sansilvestri P, Scheinecker C, et al. The Tie receptor tyrosine kinase is expressed by human hematopoietic progenitor cells and by a subset of megakaryocytic cells. Blood. 1996;87:2212–2220.
19. Lannutti BJ, Shim MH, Blake N, Reems JA, Drachman JG. Identification and activation of Src family kinases in primary megakaryocytes. Exp Hematol. 2003;31:1268–1274.
20. Kaushansky K. The molecular mechanisms that control thrombopoiesis. J Clin Invest. 2005;115:3339–3347.
21. Carter NP. Methods and strategies for analyzing copy number variation using DNA microarrays. Nat Genet. 2007;39(Suppl):S16–S21.
22. Redon R, Ishikawa S, Fitch KR, et al. Global variation in copy number in the human genome. Nature. 2006;444:444–454.
23. Jakobsson M, Scholz SW, Scheet P, et al. Genotype, haplotype and copy-number variation in worldwide human populations. Nature. 2008;451:998–1003.
24. Sebat J, Lakshmi B, Troge J, et al. Large-scale copy number polymorphism in the human genome. Science. 2004;305:525–528.
25. Raghavan M, Lillington DM, Skoulakis S, et al. Genome-wide single nucleotide polymorphism analysis reveals frequent partial uniparental disomy due to somatic recombination in acute myeloid leukemias. Cancer Res. 2005;65:375–378.
26. Kralovics R, Guan Y, Prchal JT. Acquired uniparental disomy of chromosome 9p is a frequent stem cell defect in polycythemia vera. Exp Hematol. 2002;30:229–236.

Supplementary data associated with this article can be found, in the online version, at doi:10.1016/j.exphem.2008.06.006.